Int. J. Electrochem. Sci., 17 **(2022)** Article Number: 22107, doi: 10.20964/2022.10.14

International Journal of
ELECTROCHEMICAL
SCIENCE
www.electrochemsci.org

Electrochemical Immunosensing Based on Signal Amplification Strategy for alpha-fetoprotein Detection

Junfeng Li[1], *Hui Xing*, *Peng Jin*[3], *Mingyan Li*[3], *Haiyan Liu*[3,*]

[1] Interventional Division, Second Affiliated Hospital of Shandong First Medical University, Taian, Shandong 271000, China
[2] Interventional Oncology Department, Affiliated Hospital of Weifang Medical College, Weifang, Shandong 261035, China
[3] Oncology Department, Second Affiliated Hospital of Shandong First Medical University, Taian, Shandong 271000, China
[*]E-mail: haiyanliu6236830@163.com

Received: 1 May 2022 / *Accepted:* 4 June 2022 / *Published:* 10 September 2022

Alpha-fetoprotein (AFP) is an important tumor biomarker used in cancer diagnosis. I We present an electrochemical immunosensor for highly sensitive AFP detection in this work. A commercial glassy carbon electrode was used as the working electrode. Chitosan-modified gold nanoparticles (CS-AuNPs) were synthesized by wet chemistry along with graphene oxide (GO) for the surface modification of the glassy carbon electrode. The modified electrodes can efficiently sequester anti-AFP, and by antigen-antibody specific binding, the electrodes can be applied for highly sensitive sensing of AFP. after optimization of various parameters, the proposed sensor can provide linear detection of AFP in the range of 0.1 to 100 ng/mL. The limit of detection can be calculated to be 0.041 ng/mL. In addition, the proposed immunosensor exhibited an excellent anti-interference property.

Keywords: Alpha-fetoprotein; Electrochemical immunoassay; Chitosan; AuNPs; Nanocomposite

1. INTRODUCTION

Alpha-fetoprotein (AFP), an oncogenic glycoprotein, is a polypeptide chain consisting of 591 amino acid residues and is significant component of embryonic plasma proteins [1,2]. It is also the only widely used serum marker for diagnosing primary hepatocellular carcinoma (HCC) in clinical practice. In general, the average concentration of AFP in the blood of a healthy human is ≤ 20ng/mL. If its levels are elevated in adult plasma, it may be an early sign of hepatocellular carcinoma and teratoma. Once a person develops liver cancer, the plasma level of AFP will rise sharply [3–5]. Therefore, as one of the

internationally recognized tumor markers, the monitoring of AFP is of great value in clinical tumor diagnosis.

Traditional immunoassay methods for AFP such as immunoradiometric assay, immunoturbidimetric assay, single radioimmunodiffusion assay and enzyme-linked immunoabsorption assay (ELISA) have some limitations [6–9]. Radiation hazards, complex processing steps and long analysis times have limited the practical application and development of traditional immunoassays. In contrast, immunosensors have incomparable advantages such as simplicity, separation-free, direct monitoring as well as small size and short time consumption [10–13]. Therefore, the immunosensor detection of AFP is an important direction for development. Among them, electrochemical immunosensors have been extensively investigated in recent years due to their low device cost, easy operation and high response sensitivity [14–19].

Electrochemical immunosensors are analytical methods that combine immunological techniques with electrochemical detection techniques. It is one of the earliest studies, most diverse and more mature branches of immunosensors. It consists of a molecular recognition substance (antigen, antibody) and a transducer (electrode), and performs analytical measurement of the analyte by converting the concentration of the substance to be measured into an electrochemical signal [20–25]. A Electrochemical immunosensors can be divided into a current, capacitive, impedance, and potentiometric types according to the detection method. Among them, potentiometric and capacitive type immunosensors are label-free, and current type (amperometric) immunosensors are the most maturely studied [26–30].

Current-based immunosensors detect changes in current due to antigen-antibody binding or secondary reactions at a constant voltage. It is mainly divided into enzyme-labeled and non-enzyme-labeled types, among which enzyme-labeled current immunosensors are more widely used. To improve its sensitivity, specificity and speed of detection, complexes of different metals and their oxide nanoparticles are often used to modify the electrodes [31–35]. On the other hand, it is also possible to catalyze the conversion of substrates into electroactive substances using different electron mediators and labeled enzymes [36,37].

As another form of carbon nanomaterials, graphene and doped graphene also have more applications in electrochemical immunosensing. Su et al. [38] detected AFP by immobilizing HRP conjugates with AFP (HRP-anti-AFP) on graphene and functionalized gold nanomimetic interfaces. (HRP-anti-AFP) method for AFP detection. The detection range of the sensor was 1.0 to 10 ng/mL with a detection limit of 0.7 ng/mL. The intra- and inter-batch coefficients of variation of less than 10%. Wei et al. [39] established a novel electrochemical immunosensor for AFP detection by immobilizing AFP antibodies on graphene sheets and Thi-modified glassy carbon electrodes. It has a detection range of 0. 05 to 2. 00 ng/mL and a detection limit of 5.77 pg/mL. Du et al. [40] used graphene sheets as a platform for functionalized nanomicrospheres carbon labeled with horseradish peroxidase secondary antibody (HRP-Ab2). It has a linear range of 0. 05 to 6 ng/mL and a detection limit of 0. 02 ng/mL. Huang et al. [41] constructed a current-based immunosensor to detect of AFP with a detection limit of 0. 1 ng/mL using amino-functionalized graphene and nanogold complexes modified with carbon ionic liquid electrodes.

In experimental studies of electrochemical immunosensors, metal and compound nanoparticles, magnetic (or non-magnetic) metal compound nanoparticles are commonly used as electrode

modification materials. This enhances biocompatibility and sequestration of biomolecules, which improves the biosensor's measurement sensitivity. Zhuo et al. [42] constructed an ultra-sensitive and reproducible electrochemical immunosensor with dual enzyme functionalized Au-PB-Fe_3O_4 triple-layered magnetic nuclei nanoparticles for the first time. It is composed of Fe_3O_4 magnetic core, PB and gold core. The results indicate that the multilabeled Au-PB-Fe_3O_4 nanoparticles exhibit good redox electrochemical activity, as well as high analytical activity, and may be regenerated by external magnetic fields. Gan et al. [43] prepared a novel magnetic nanoprobe by immobilizing an AFP antibody on a glassy carbon electrode modified by a nano-Fe_3O_4 (core)/ZrO_2 (shell)-nanoAu-polylysine composite membrane. The linear range of the sensor was 0.05-10 ng/mL, and the detection limit was 0.01 ng/mL. Gan et al. [44] also constructed a DNA/(ZMPs-HRP-AFPAb2) sandwich-type electrochemical immunosensor to detect of AFP using magnetic DNA nanoprobes on the surface of AuNPs-modified glassy carbon electrodes. Tang et al. [45] constructed another novel AFP immunosensor by first immobilizing AFP antibody on the surface of core-shell type Fe_2O_3/Au magnetic nanoparticles and then adsorbing it on the surface of carbon paste electrode, which has a linear range of 1 to 80 ng/mL and a detection limit of 0.5 ng/mL. Wang et al. [46] used $COFe_2O_4$ covalently bound to trimethoxymethylsilane, and then AuNPs were absorbed on the $COFe_2O_4$-MPS surface through gold-sulfur bonding to form a core-shell composite nanomaterial, after which AFP antibodies were immobilized on the nanogold surface. Biomolecules doped with magnetic nanoparticles can be effectively separated by the action of an external magnetic field. The sensor has a wide linear range: 0.8 to 120.0 ng/mL, with a detection limit of 0.3 ng/mL. In this paper, chitosan (CS)-AuNPs@graphene oxide (GO) composites were prepared by electrochemical method by electrodeposition of CS-AuNPs on the surface of GO. The adsorption of AuNPs on proteins and the binding of -OH of CS molecules to -NH_2 and -COOH of protein molecules were used to construct an electrochemical immunosensor for the rapid detection of AFP.

2. EXPERIMENTAL

2.1. Reagents

HCl (AR), KH_2PO_4(AR), KCl (AR), $Na_2HPO_4 \cdot 12H_2O$ (AR), NaOH (AR), $K_3[Fe(CN)_6]$ (AR), $K_4[Fe(CN)_6]$ (AR), $K_4[Fe(CN)_6]$ (AR) and C_2H_5OH were purchased from Sinopharm Chemical Reagent Co. CS (AR) was purchased from Shanghai Blue Season Technology Development Co. $HAuCl_4$ (Au≥47.5%) was purchased from Aladdin Reagent (Shanghai) Co. GO aqueous solution was purchased from Nanjing Pioneer Nano Technology Development Co. AFP and anti-AFP were purchased from Shanghai Yubo Biotechnology Co.(0.01M PBS, pH 7.4 with 10 mg/mL BSA and 0.1% sodium azide).

Weigh 50.2 mg of CS solid, dissolve and prepare 500 mg/L of CS solution (solvent is 1% acetic acid), and store at room temperature under seal. Weigh 25 mg of $HAuCl_4$ solid in 100 mL of deionized water to prepare 250 mg/L of $HAuCl_4$ solution and refrigerate it away from light.

2.2. Electrochemical sensor fabrication

GO/GCE: 1 mg/mL of GO was modified onto the surface of GCE electrodes by drop coating, dried and ready for use.

CS-AuNPs/GO/GCE: CS solution (1% acetic acid as solvent) was co-mixed with $HAuCl_4$ solution in a 1:1 volume ratio. CS-AuNPs/GO/GCE was obtained by electrodeposition on GO/GCE at a voltage of 1.5 V for 3 min, and then dried and stored.

Anti-AFP/CS-AuNPs/GO/GC: 10 μg/mL anti-AFP was modified on the dried CS-Au NPs/GO/GCE surface. BSA was added dropwise to the electrode surface with 1% bovine serum protein (BSA) to seal the inactive sites on the electrode. Next, the modified electrode was incubated with different concentrations of AFP under optimal conditions.

2.3. Electrochemical measurements

The electrochemical experiments were carried out using a conventional three-electrode system and were performed by a CHI 660A electrochemical workstation (Shanghai C&H, China). The reference electrode is a saturated glycury electrode (SCE). The auxiliary electrode was a platinum wire (Pt). The working electrode is a fully modified GC electrode. Differential pulse voltammetry (DPV) detection is performed at a pulse frequency of 50 mV, an amplitude width of 50 ms, and a scan range of -0.2 V to +0.6 V. Impedance curves (EIS Nyquist) were performed in 0.1 mol/L PBS (pH = 7.4) electrolyte containing 10 mM $[Fe(CN)_6/Fe(CN)_6]^{3-/4-}$ and 0.1 M KCl in the frequency range of 1 Hz to 100 kHz.

3. RESULTS AND DISCUSSION

FTIR spectra were used to characterize the functional groups contained on the surface of CS-AuNPs. As shown in Figure 1, the peaks located 3405 cm^{-1} and 3133 cm^{-1} can be ascribed to the stretching vibration of free N-H [47]. The peaks at 1712 cm^{-1} and 1615 cm^{-1} originate from the hydroxyl stretching vibration and the shear vibration absorption of NH_2 [48], respectively, which indicate that the amide bond is generated by the combination of amino and carboxyl groups in the reaction. The peaks located at 2950 cm^{-1} and 2844 cm^{-1} originate from the asymmetric and symmetric stretching vibrations of -CH2, and the absorption peak at 1402 cm^{-1} from the bending vibrations of C-H. The FTIR results indicate the successful synthesis of CS-AuNPs [49].

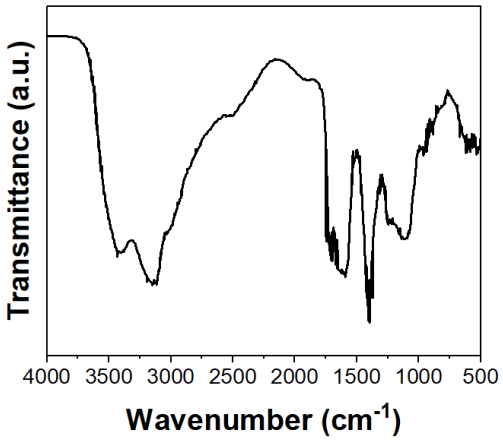

Figure 1. FTIR spectrum of CS-AuNPs.

The surface composition of the CS-AuNPs nanocomposite was measured by XPS (Figure 2). It can be seen from the figure that the composite contains mainly four elements C, N, O and Au. the appearance of Au 4f double peaks (83.3 eV and 87.8 eV) is consistent with the Au0 valence state and also the peaks of Au $4d_{3/2}$ (353 eV) and Au4d5/3 (335 eV) gold in other valence states, these results indicate the formation of nanogold on the nanocomposite [50].

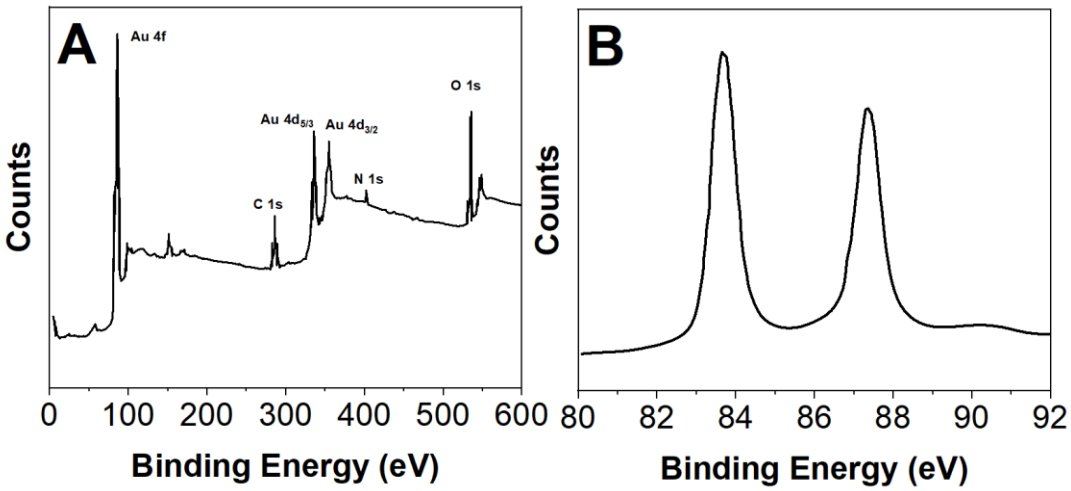

Figure 2. (A) Full XPS spectrum and (B) Au 4f spectrum of CS-AuNPs.

The construction process of the CS-AuNPs nanocomposite modified electrochemical immunosensor is shown in Figure 3. The CS-AuNPs nanocomposite was immobilized on the electrode surface by a drop coating method, and anti-AFP was immobilized by electrostatic interaction through the nanogold exposed on the composite surface. Then, BSA was used to seal the unbound sites of the antibody to avoid non-specific adsorption. During detection, AFP can be immobilized on the electrode

surface by immunoreactivity, which is manifested by a decrease in current. Since the decrease in current is proportional to the amount of AFP immobilized, the quantitative detection of AFP can be achieved.

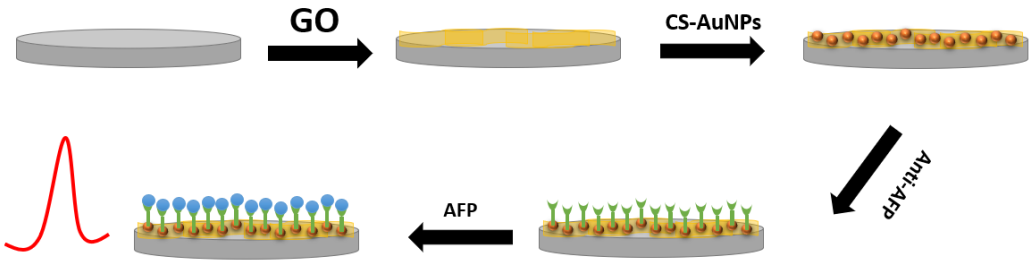

Figure 3. Schematic diagram of AFP immunosensor fabrication and detection.

Figure 4 shows the electrochemical impedance plots during the construction of the AFP immunosensor. The small radius of the semicircle formed by the GO/GCE impedance curve indicates that GO/GCE has a low charge transfer impedance in the electrolyte solution. When the CS-AuNPs was successfully immobilized on the surface of GO/GCE, the electrode resistance decreased, indicating that the electrodeposited gold nanoparticles have good conductivity, which improved the conductivity of the electrode to some extent [51]. Then it was compounded with anti-AFP to form anti-AFP-CS-AuNPs/GO. The resistance was further increased because anti-AFP was not conductive. This indicates that the anti-AFP modification successfully blocks electron transfer and reduces the conductivity of the electrode [52]. In the same way, when BSA and AFP have applied dropwise to the electrode afterwards, the resistance of the electrode to electron transfer increased in turn, resulting in BSA-anti-AFP-CS-AuNPs/GO and AFP-BSA-CS-AuNPs/GO, respectively. Anti-AFP-CS-Au NPs/GO.

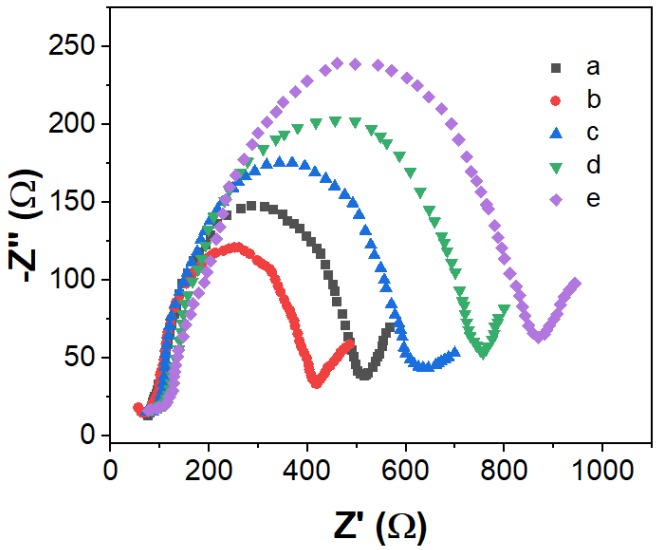

Figure 4. EIS plots of (a) GO/GCE, (b) CS-AuNPs/GO/GCE, (c) anti-AFP/CS-AuNPs/GO/GCE, (d) BSA/anti-AFP/CS-AuNPs/GO/GCE and (e) AFP/BSA/anti-AFP/CS-AuNPs/GO/GCE.

Figure 5A shows the plot between the same test solution (10 mM $[Fe(CN)_6]^{3-/4-}$) and the DPV peak current of the immunosensor at different pH values. In all subsequent experiments with optimized conditions, we chose AFP at a concentration of 40 ng/mL for condition exploration. As can be seen from the graph, the peak current value of DPV increases and then decreases, and it can be seen that the peak current value of DPV has a maximum at pH=7.4. Highly acidic or strongly alkaline environments can destroy the stability and activity of immobilized proteins [53]. Therefore, pH = 7.4 was chosen as the optimal pH for detecting AFP antigen.

The binding of antigen-antibody takes some time to proceed, therefore, the length of incubation time also directly affects the degree of antigen-antibody binding. Figure 5B shows the relationship between the peak current of DPV and the antigen-antibody incubation time. The response current decreases with increasing incubation time. When the incubation time exceeds 50 min, the current response decreases and then stabilizes [6]. This indicates that the binding ability of antigen and antibody gradually saturates. Therefore, we choose 50 min as the optimal incubation time.

The temperature also influenced the protein activity and the degree of biochemical reaction, and the incubation temperature also had an important effect on the binding of antigen and antibody. The overall trend of the analysis in Figure 5C is that the peak current of DPV decreases and then increases as the temperature increases. 35 ℃ is when the current decreases because the protein activity increases gradually with the increase of temperature. The lowest peak current value was observed at 35 ℃, indicating that the antigen-antibody binding level was optimal at this time. The peak current tends to increase when the temperature exceeds 35 ℃. This is because the continuous increase in temperature will lead to a decrease in protein activity, which will lead to the gradual increase of current due to the inactivation of some proteins by the high temperature [10]. Therefore, 35 ℃ is the optimal temperature for the immune response in this experiment. However, considering the activity of biomolecules and the lifetime of the sensor, we chose 37 °C as the optimal incubation temperature.

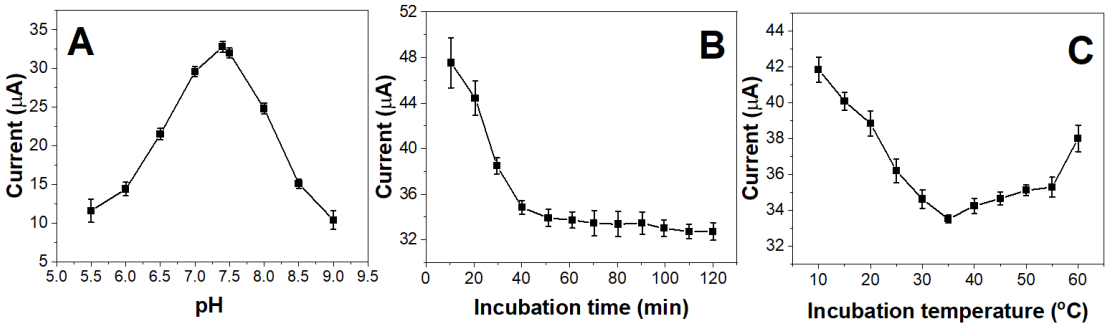

Figure 5. The effect of (A) pH, (B) incubation time, (C) incubation temperature in the current response of AFP/BSA/anti-AFP/CS-AuNPs/GO/GCE in 10 mM $[Fe(CN)_6]^{3-/4-}$

In order to evaluate the performance of the prepared immunosensor, the electrochemical response of the sensor to different concentrations of antigen was investigated under the optimal experimental conditions, and the relationship between the antigen concentration and the response current of the

immunosensor was sought. As shown in Figure 6A, the DPV test curves at different concentrations of AFP (0.1 to 100 ng/mL), the peak current values decreased continuously with the increase of AFP concentration and showed a linear variation. This is because as the concentration of AFP increases, the number of antibodies bound to AFP also increases. The formed antigen-antibody complex acts as an inert kinetic barrier to ferricyanide electron transfer, so that the current hindrance it generates is reflected in a regular linear decrease in peak current magnitude [54]. The current variation of the CS-Au NPs/ GO/GCE-based immunosensor was linearly proportional to the AFP concentration in the range of 0.1 to 100 ng/mL.

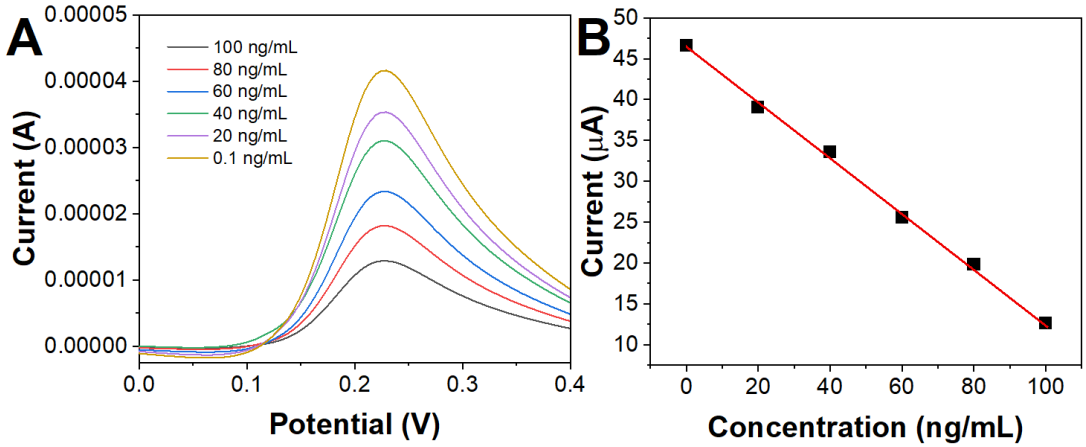

Figure 6. (A) DPV curves of BSA/anti-AFP/CS-AuNPs/GO/GCE towards 0.1 ng/mL, 20 ng/mL, 40 ng/mL, 80 ng/mL and 100 ng/mL AFP. (B) Calibration curve of immunosensor in different concentrations of AFP.

Table 1. Sensing performance of the BSA/anti-AFP/CS-AuNPs/GO/GCE and other electrochemical sensors for AFP detection.

Sensor	Linear detection range	Limit of detection	Reference
MoS_2@Cu_2O-Au	0.1–50 ng/mL	0.037 ng/mL	[55]
BSA/AFP-Ab/AuNPs/PGNR/GCE	5–60 ng/mL	1.00 ng/mL	[56]
BSA/AFP-Apt/GO/GCE	0.1-100 ng/mL	0.003 ng /mL	[57]
BSA/AFP-Apt/PtNPs/GO-COOH/SPGE	3–30 ng/mL	1.22 ng /mL	[58]
BSA/anti-AFP/CS-AuNPs/GO/GCE	0.1-100 ng/mL	0.041 ng /mL	This work

The calculated detection limit was 0.041 ng/mL (signal-to-noise ratio S/N = 3). Figure 6B shows the calibration curve for AFP determination with the constructed immunosensor under optimal experimental conditions. The detection range and detection limit are two important indicators for evaluating the electrochemical immunosensor. We compared the performance of this sensor with other label-free immunosensors based on carbon nanomaterials. The data in Table 1 shows that AFP/BSA/anti-

AFP/CS-AuNPs/GO/GCE can compete with many other sensors in terms of the linear range of detection and detection limit.

To test the response of the constructed immunosensors to interferences or cross-recognition, we evaluated the specificity of the immunosensors using some possible interfering factors such as carcinoembryonic antigen (CEA), CA199, CA125 and CA153 [59] (Figure 7). Incubation of the immunosensor with 20 ng/mL AFP in the presence of 60 ng/mL interfering agent revealed that the response currents obtained did not differ significantly in response signal between pure AFP and AFP with interfering substances, indicating that the immunosensor has good resistance to interference for the detection of AFP.

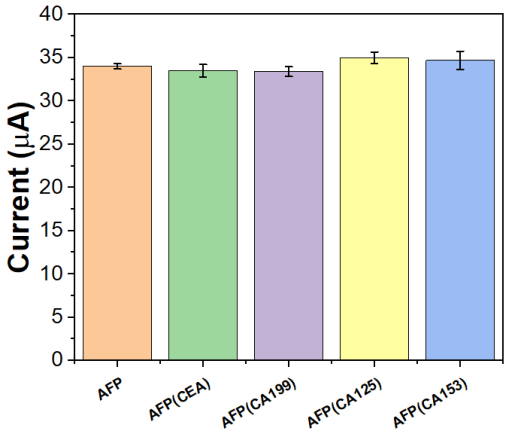

Figure 7. Anti-interference property of the BSA/anti-AFP/CS-AuNPs/GO/GCE towards AFP, AFP+CEA, AFP+CA199, AFP+CA125 and AFP+CA153.

4. CONCLUSION

In conclusion, in this paper, CS-AuNPs/GO composites were successfully prepared and used to construct electrochemical immunosensors for the rapid and sensitive detection of AFP. The results showed that the CS-Au NPs/GO modified AFP biosensor exhibited good electrochemical performance with short incubation time, simple electrode construction, good interference resistance and good stability. These are attributed to the large comparative area, good biocompatibility and conductivity of CS-Au NPs/ GO. Based on this, our constructed sensor is well suited for the detection of AFP, which is linearly detected in the range of 0.1 to 100 ng/mL. The detection limit was calculated to be 0.041 ng/mL, which can be helpful in the clinical detection of AFP.

References

1. C. Sun, L. Pan, L. Zhang, J. Huang, D. Yao, C.-Z. Wang, Y. Zhang, N. Jiang, L. Chen, C. Yuan, *Analyst*, 144 (2019) 6760–6772.
2. S. Yan, Y. Yue, L. Zeng, L. Su, M. Hao, W. Zhang, X. Wang, *Front. Chem.*, 9 (2021) 220.
3. S. Wang, M. Wang, C. Li, H. Li, C. Ge, X. Zhang, Y. Jin, *Sens. Actuators B Chem.*, 311 (2020)

127919.
4. X. Wang, J. Ji, P. Yang, X. Li, Y. Pang, P. Lu, *Talanta*, 243 (2022) 123328.
5. Z. Zhang, M. Peng, D. Li, J. Yao, Y. Li, B. Wu, L. Wang, Z. Xu, *Front. Chem.*, 9 (2021) 702.
6. F. Pei, P. Wang, E. Ma, Q. Yang, H. Yu, J. Liu, H. Yin, Y. Li, Q. Liu, Y. Dong, *J. Electroanal. Chem.*, 835 (2019) 197–204.
7. S. Zhao, N. Liu, W. Wang, Z. Xu, Y. Wu, X. Luo, *Biosens. Bioelectron.*, 190 (2021) 113466.
8. Y. Zheng, D. Wang, X. Li, Z. Wang, Q. Zhou, L. Fu, Y. Yin, D. Creech, *Biosensors*, 11 (2021) 403.
9. H. Karimi-Maleh, Y. Orooji, F. Karimi, M. Alizadeh, M. Baghayeri, J. Rouhi, S. Tajik, H. Beitollahi, S. Agarwal, V.K. Gupta, *Biosens. Bioelectron.* (2021) 113252.
10. X. Yang, C. Zhao, C. Zhang, K. Wen, Y. Zhu, *Sens. Actuators B Chem.*, 323 (2020) 128666.
11. D.H. Kim, H.G. Oh, W.H. Park, D.C. Jeon, K.M. Lim, H.J. Kim, B.K. Jang, K.S. Song, *Sensors*, 18 (2018) 4032.
12. D. Wang, D. Li, L. Fu, Y. Zheng, Y. Gu, F. Chen, S. Zhao, *Sensors*, 21 (2021) 8216.
13. H. Karimi-Maleh, A. Khataee, F. Karimi, M. Baghayeri, L. Fu, J. Rouhi, C. Karaman, O. Karaman, R. Boukherroub, *Chemosphere* (2021) 132928.
14. A. Mohammadinejad, R.K. Oskuee, R. Eivazzadeh-Keihan, M. Rezayi, B. Baradaran, A. Maleki, M. Hashemzaei, A. Mokhtarzadeh, M. de la Guardia, *TrAC Trends Anal. Chem.*, 130 (2020) 115961.
15. Y. Li, J. Yuan, S. Zhan, J. Hu, Y. Guo, L. Ding, X. Huang, Y. Xiong, *Sens. Actuators B Chem.*, 341 (2021) 130030.
16. X. Liao, X. Wang, P. Li, S. Chen, M. Zhang, L. Mei, Y. Qi, C. Hong, *Sens. Actuators B Chem.*, 344 (2021) 130258.
17. J. Zhou, Y. Zheng, J. Zhang, H. Karimi-Maleh, Y. Xu, Q. Zhou, L. Fu, W. Wu, *Anal. Lett.*, 53 (2020) 2517–2528.
18. S. Wei, X. Chen, X. Zhang, L. Chen, *Front. Chem.*, 9 (2021) 697.
19. H. Karimi-Maleh, F. Karimi, L. Fu, A.L. Sanati, M. Alizadeh, C. Karaman, Y. Orooji, *J. Hazard. Mater.*, 423 (2022) 127058.
20. L. Fu, A. Yu, G. Lai, *Chemosensors*, 9 (2021) 282.
21. Y. Zheng, S. Mao, J. Zhu, L. Fu, N. Zare, F. Karimi, *Food Chem. Toxicol.*, 164 (2022) 113019.
22. Y. Shen, S. Mao, F. Chen, S. Zhao, W. Su, L. Fu, N. Zare, F. Karimi, *Food Chem. Toxicol.*, 163 (2022) 112960.
23. D. Sun, H. Li, M. Li, C. Li, L. Qian, B. Yang, *Biosens. Bioelectron.*, 132 (2019) 68–75.
24. H. Sha, Y. Wang, Y. Zhang, H. Ke, X. Xiong, N. Jia, *Sens. Actuators B Chem.*, 277 (2018) 157–163.
25. H. Karimi-Maleh, M. Alizadeh, Y. Orooji, F. Karimi, M. Baghayeri, J. Rouhi, S. Tajik, H. Beitollahi, S. Agarwal, V.K. Gupta, S. Rajendran, S. Rostamnia, L. Fu, F. Saberi-Movahed, S. Malekmohammadi, *Ind. Eng. Chem. Res.*, 60 (2021) 816–823.
26. S. Li, X. Liu, S. Liu, M. Guo, C. Liu, M. Pei, *Anal. Chim. Acta*, 1141 (2021) 21–27.
27. G. Li, S. Li, Z. Wang, Y. Xue, C. Dong, J. Zeng, Y. Huang, J. Liang, Z. Zhou, *Anal. Biochem.*, 547 (2018) 37–44.
28. Y. Zheng, X. Li, F. Han, L. Fu, J. Sun, *Int J Electrochem Sci*, 16 (2021) 211136.
29. W. Ye, Y. Zheng, P. Zhang, B. Fan, Y. Li, L. Fu, *Int J Electrochem Sci*, 16 (2021) 211041.
30. H. Karimi-Maleh, H. Beitollahi, P.S. Kumar, S. Tajik, P.M. Jahani, F. Karimi, C. Karaman, Y. Vasseghian, M. Baghayeri, J. Rouhi, *Food Chem. Toxicol.* (2022) 112961.
31. M. Jin, J. Liu, W. Wu, Q. Zhou, L. Fu, N. Zare, F. Karimi, J. Yu, C.-T. Lin, *Chemosphere*, 300 (2022) 134599.
32. L. Fu, X. Zhang, S. Ding, F. Chen, Y. Lv, H. Zhang, S. Zhao, *Curr. Pharm. Anal.*, 18 (2022) 4–13.
33. R. Duan, X. Fang, D. Wang, *Front. Chem.*, 9 (2021) 361.

34. H. Karimi-Maleh, A. Ayati, R. Davoodi, B. Tanhaei, F. Karimi, S. Malekmohammadi, Y. Orooji, L. Fu, M. Sillanpää, *J. Clean. Prod.*, 291 (2021) 125880.
35. H. Karimi-Maleh, A. Ayati, S. Ghanbari, Y. Orooji, B. Tanhaei, F. Karimi, M. Alizadeh, J. Rouhi, L. Fu, M. Sillanpää, *J. Mol. Liq.*, 329 (2021) 115062.
36. Z. Li, H. Li, D. Deng, R. Liu, Y. Lv, *Anal. Chem.*, 92 (2020) 4807–4813.
37. M. Wu, Y. Yang, K. Cao, C. Zhao, X. Qiao, C. Hong, *Bioelectrochemistry*, 132 (2020) 107434.
38. B. Su, J. Tang, J. Huang, H. Yang, B. Qiu, G. Chen, D. Tang, *Electroanalysis*, 22 (2010) 2720–2728.
39. Q. Wei, K. Mao, D. Wu, Y. Dai, J. Yang, B. Du, M. Yang, H. Li, *Sens. Actuators B Chem.*, 149 (2010) 314–318.
40. D. Du, Z. Zou, Y. Shin, J. Wang, H. Wu, M.H. Engelhard, J. Liu, I.A. Aksay, Y. Lin, *Anal. Chem.*, 82 (2010) 2989–2995.
41. K.-J. Huang, D.-J. Niu, J.-Y. Sun, J.-J. Zhu, *J. Electroanal. Chem.*, 656 (2011) 72–77.
42. Y. Zhuo, P.-X. Yuan, R. Yuan, Y.-Q. Chai, C.-L. Hong, *Biomaterials*, 30 (2009) 2284–2290.
43. N. Gan, Y. Wu, F. Hu, T. Li, L. Zheng, Y. Cao, *Int J Electrochem Sci*, 6 (2011) 461–474.
44. N. Gan, L. Jia, L. Zheng, *J. Autom. Methods Manag. Chem.*, 2011 (2011) 957805.
45. D. Tang, R. Yuan, Y. Chai, *Biotechnol. Lett.*, 28 (2006) 559–565.
46. L. Wang, X. Gan, *Microchim. Acta*, 164 (2009) 231–237.
47. Y. Wang, G. Zhao, H. Wang, W. Cao, B. Du, Q. Wei, *Biosens. Bioelectron.*, 106 (2018) 179–185.
48. Y. Wu, H. Su, J. Yang, Z. Wang, D. Li, H. Sun, X. Guo, S. Yin, *J. Colloid Interface Sci.*, 580 (2020) 583–591.
49. S. Zhang, C. Zhang, Y. Jia, X. Zhang, Y. Dong, X. Li, Q. Liu, Y. Li, Z. Zhao, *Bioelectrochemistry*, 128 (2019) 140–147.
50. X. Zhao, A. Zhu, Y. Wang, Y. Zhang, X. Zhang, *Molecules*, 26 (2021) 1197.
51. N. Ma, T. Zhang, D. Fan, X. Kuang, A. Ali, D. Wu, Q. Wei, *Sens. Actuators B Chem.*, 297 (2019) 126821.
52. H. Karimi-Maleh, C. Karaman, O. Karaman, F. Karimi, Y. Vasseghian, L. Fu, M. Baghayeri, J. Rouhi, P. Senthil Kumar, P.-L. Show, S. Rajendran, A.L. Sanati, A. Mirabi, *J. Nanostructure Chem.* (2022).
53. H. Shi, L. Fu, F. Chen, S. Zhao, G. Lai, *Environ. Res.*, 209 (2022) 112747.
54. Y. Chen, X. Chen, J. Lin, Y. Zhuang, Z. Han, J. Chen, *Micromachines*, 13 (2022) 673.
55. N. Ma, T. Zhang, D. Fan, X. Kuang, A. Ali, D. Wu, Q. Wei, *Sens. Actuators B Chem.*, 297 (2019) 126821.
56. L. Jothi, S.K. Jaganathan, G. Nageswaran, *Mater. Chem. Phys.*, 242 (2020) 122514.
57. S. Yang, F. Zhang, Z. Wang, Q. Liang, *Biosens. Bioelectron.*, 112 (2018) 186–192.
58. J. Upan, N. Youngvises, A. Tuantranont, C. Karuwan, P. Banet, P.-H. Aubert, J. Jakmunee, *Sci. Rep.*, 11 (2021) 13969.
59. M. Force, G. Park, D. Chalikonda, C. Roth, M. Cohen, D. Halegoua-DeMarzio, H.-W. Hann, *Viruses*, 14 (2022) 775.